Electronic Supplementary Information

New tetrathiafulvalene fused-naphthalene diimides for solution processible and air stable *p*-type and ambipolar organic semiconductors

Luxi Tan, Yunlong Guo, Yang Yang, Guanxin Zhang,* Deqing Zhang,* Gui Yu, Wei Xu, Yunqi Liu

Beijing National Laboratory for Molecular Sciences, Organic Solids Laboratory, Institute of Chemistry, Chinese Academy of Sciences, Beijing 100190, China.

E-mail: dqzhang@iccas.ac.cn

Contents

1. **General information for synthesis and characterization…….S2**
2. **TGA analysis of 1-6…….S3**
3. **The absorption spectra of *N,N'*-hexyl NDI, 2, 3, 5, 6 and 13……S5**
4. **Cyclic voltammograms of *N,N'*-hexyl NDI, 2, 3, 5, 6 and 13……S7**
5. **The performance data of OFETs with 4-6 using unmodified Au as electro…S9**
6. **XRD patterns and AFM images of 1, 2 and 4, 6……S10**
7. **DFT calculation data……...……S11**
8. **^{1}H NMR and ^{13}C NMR spectra of 1-8……...S15**
9. **The absorption spectra of compounds 2 and 4 after UV light irradiantion.S21**

1. General information for synthesis and characterization

Chemicals were purchased form Alfa-Aesar, Sigma-Aldrich and used without further purification. Solvents and other common reagents were obtained from Beijing Chemical Co.. ^{1}H NMR (400 MHz) and ^{13}C NMR (100 MHz) spectra were obtained on a Bruker DMX-400 NMR Spectrometer using tetramethylsilane as internal standard. Elemental analysis was performed on a Carlo Erba model 1160 elemental analyzer. MALDI-TOF MS were recorded with BEFLEX III spectrometer. Solution and thin films (which were frabricated on a quartz plate) absorption spectra were measured with JASCO V-570 UV-Vis spectrophtometer. TGA-DTA measurements were carried out on a SHIMADZU DTG-60 instruments under a dry nitrogen flow, heating from room temperature to 500 °C, with a heating rate of 10 °C/min. Cyclic voltammetric measurements were carried out in a conventional three-electrode cell using Pt wires of 2 mm diameter as working and counter electrodes, and an Ag/AgCl reference electrode on a computer-controlled CHI660C instruments at room temperature. X-ray diffraction (XRD) measurements were carried out in the reflection mode at room temperature, using a 2-kW Rigaku X-ray diffraction system. The molecular structures of the compounds were calculated with the DFT method at B3LYP/6-31G(d, p) level. All calculations were performed with the Gaussian 09 program.

2. TGA analysis of compounds 1-6

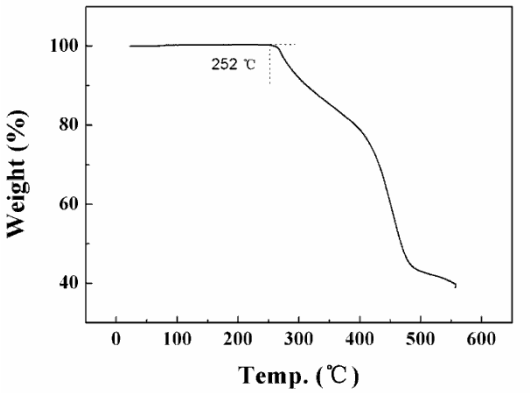

Figure S1. TGA curve of **1**.

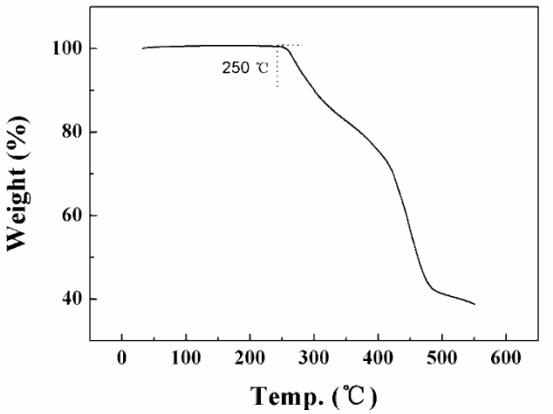

Figure S2. TGA curve of **2**.

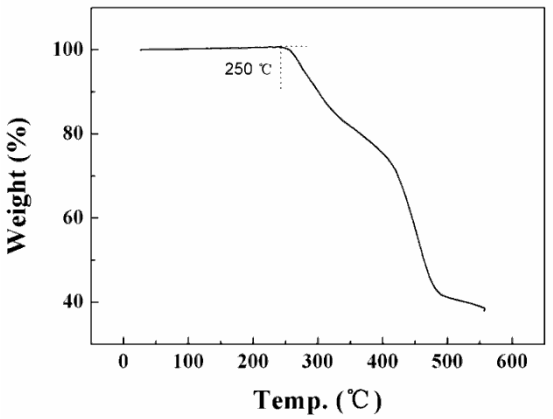

Figure S3. TGA curve of **3**.

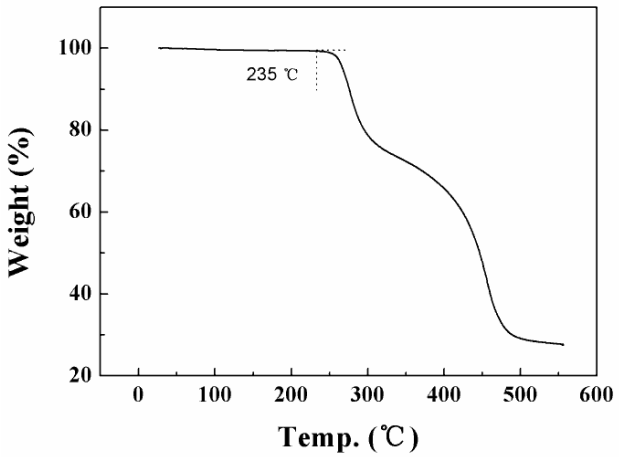

Figure S4. TGA curve of **4**.

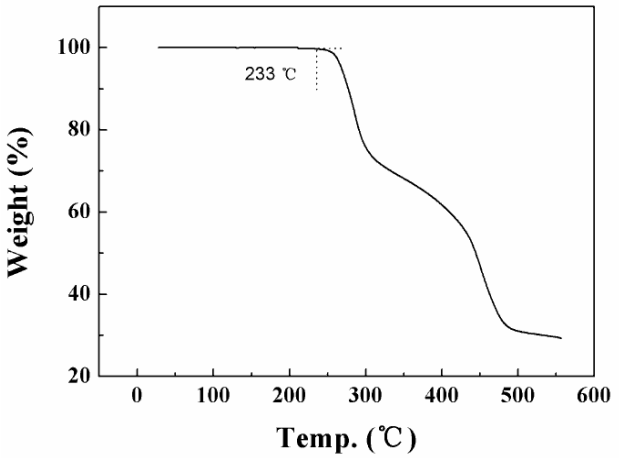

Figure S5. TGA curve of **5**

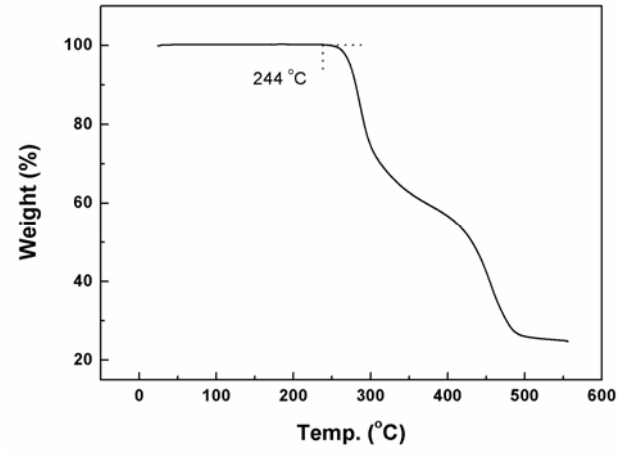

Figure S6. TGA curve of **6**.

3. UV-Vis absorption spectra of *N,N'*-hexyl NDI, 2, 3, 5, 6 and 13

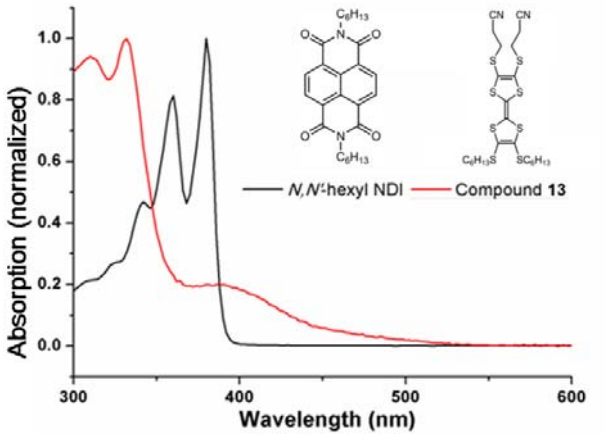

Figure S7. Absorption spectra of *N,N'*-hexyl NDI (1.0×10^{-4} M) and compound **13** (1.0×10^{-4} M) in CH_2Cl_2.

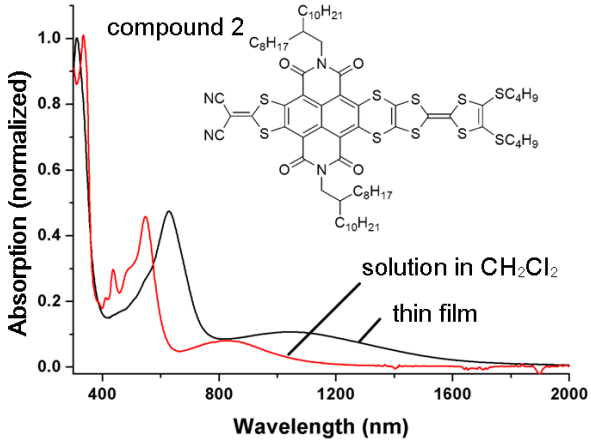

Figure S8. Absorption spectra of compound **2** in solution ($\varepsilon_{550nm} = 1.0 \times 10^4$ M^{-1} cm^{-1} in CH_2Cl_2) and thin film.

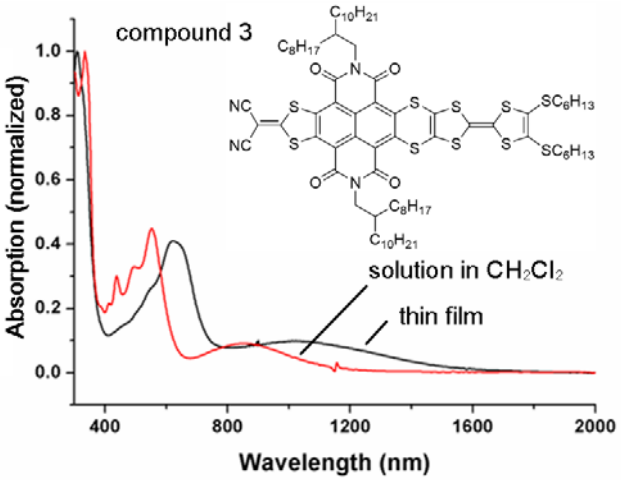

Figure S9. Absorption spectra of compound **3** in solution ($\varepsilon_{550nm} = 1.0 \times 10^4$ M^{-1} cm^{-1} in CH_2Cl_2) and thin film.

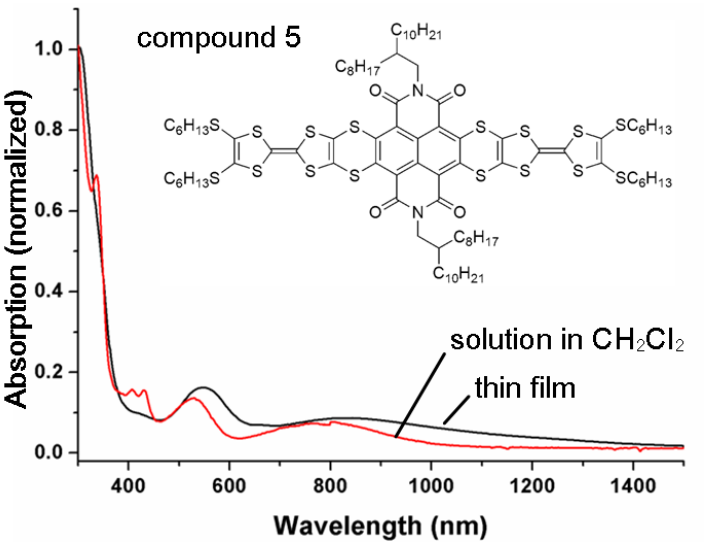

Figure S10. Absorption spectra of compound **5** in solution ($\varepsilon_{530nm} = 8.8 \times 10^3$ M^{-1} cm^{-1} in CH_2Cl_2) and thin film.

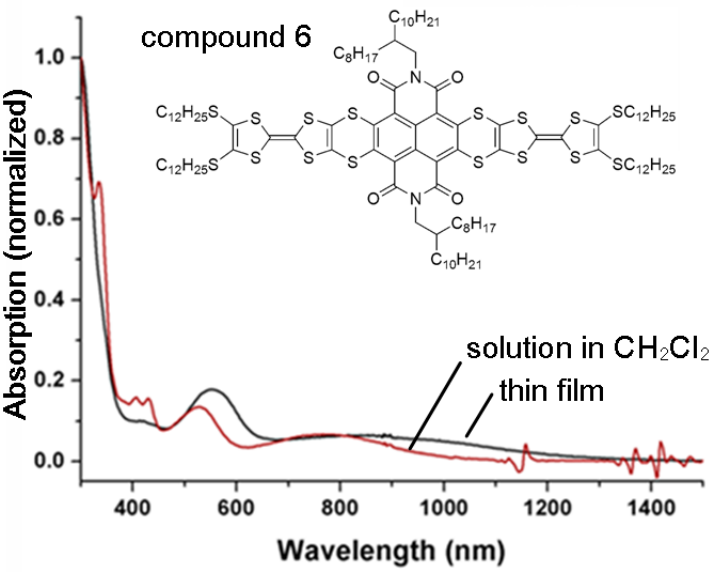

Figure S11. Absorption spectra of compound **6** in solution ($\varepsilon_{530nm} = 8.9 \times 10^3$ M^{-1} cm^{-1} in CH_2Cl_2) and thin film.

4. Cyclic voltammograms of of *N,N'*-hexyl NDI, 2, 3, 5, 6 and 13

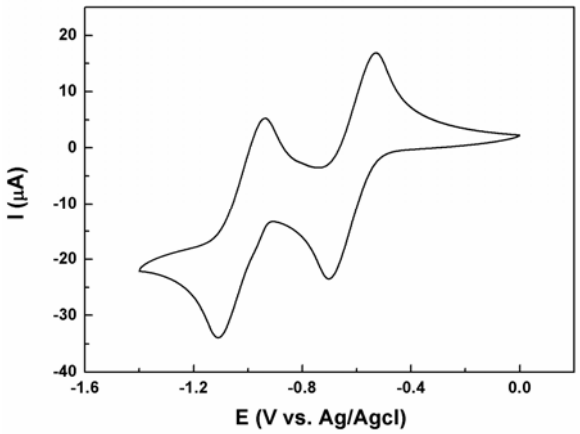

Figure S12. Cyclic voltammogram of *N,N'*-hexyl NDI in CH_2Cl_2 (1.0×10^{-3} M) at a scan rate of 100 mV s^{-1}, with Pt as the working and counter electrodes and Ag/AgCl electrode (saturated KCl) as the reference electrode, and *n*-Bu_4NPF_6 (0.1 M) as supporting electrolyte.

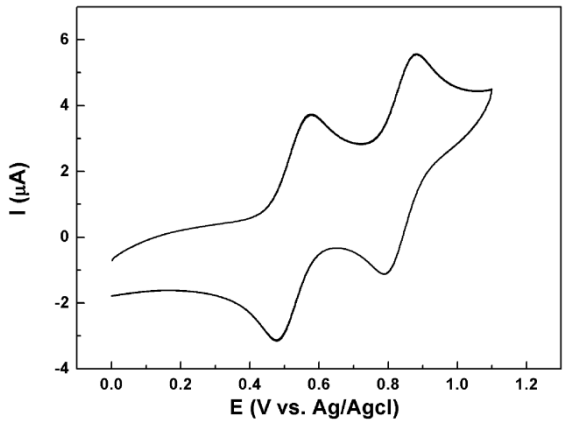

Figure S13. Cyclic voltammograms of compound **13** in CH_2Cl_2 (1.0×10^{-3} M) at a scan rate of 100 mV s^{-1}, with Pt as the working and counter electrodes and Ag/AgCl electrode (saturated KCl) as the reference electrode, and *n*-Bu_4NPF_6 (0.1 M) as supporting electrolyte.

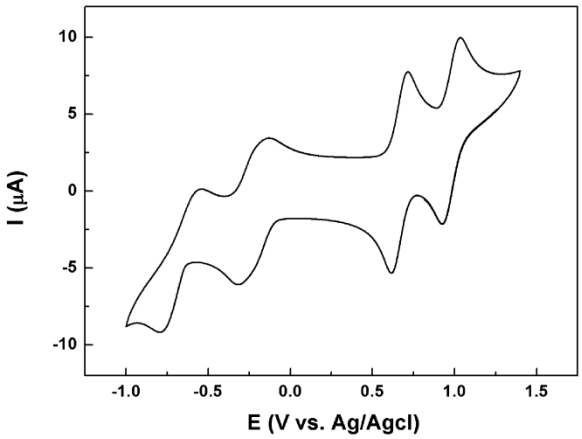

Figure S14. Cyclic voltammograms of compound **2** in CH_2Cl_2 (1.0×10^{-3} M) at a scan rate of 100 mV s^{-1}, with Pt as the working and counter electrodes and Ag/AgCl electrode (saturated KCl) as the reference electrode, and *n*-Bu_4NPF_6 (0.1 M) as supporting electrolyte.

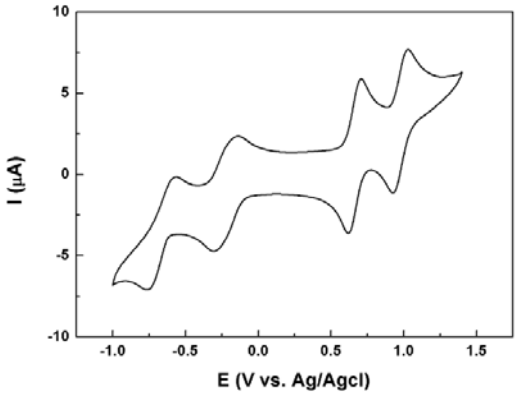

Figure S15. Cyclic voltammograms of compound **3** in CH_2Cl_2 (1.0×10^{-3} M) at a scan rate of 100 mV s^{-1}, with Pt as the working and counter electrodes and Ag/AgCl electrode (saturated KCl) as the reference electrode, and *n*-Bu_4NPF_6 (0.1 M) as supporting electrolyte.

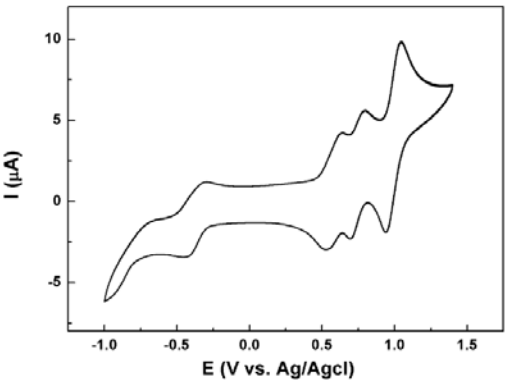

Figure S16. Cyclic voltammograms of compound **5** in CH_2Cl_2 (1.0×10^{-3} M) at a scan rate of 100 mV s^{-1}, with Pt as the working and counter electrodes and Ag/AgCl electrode (saturated KCl) as the reference electrode, and *n*-Bu_4NPF_6 (0.1 M) as supporting electrolyte.

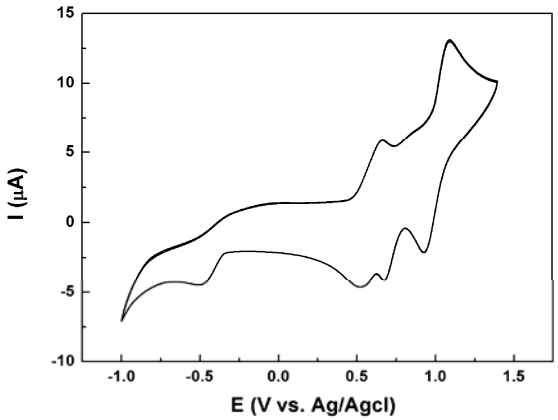

Figure S17. Cyclic voltammograms of compound **6** in CH_2Cl_2 (1.0×10^{-3} M) at a scan rate of 100 mV s^{-1}, with Pt as the working and counter electrodes and Ag/AgCl electrode (saturated KCl) as the reference electrode, and *n*-Bu_4NPF_6 (0.1 M) as supporting electrolyte.

5. The performance data of OFETs with 4-6 using unmodified Au as electrodes

Table S1. The hole mobilities (μ_h), threshold voltages (V_{th}), and on/off ratios ($I_{on/off}$) for bottom contact OFET devices based on thin-films of **4-6** with unmodified Au as electrodes at different annealing temperatures.[a]

Compd.	Temp./°C	μ_h / cm^2 V^{-1} s^{-1}	V_{th}/V	$I_{on/off}$
4	25	$3.8–4.0 \times 10^{-4}$	-5–1	10^2
	120	$0.8–1.0 \times 10^{-3}$	-6–1	10^2
	140	$1.4–1.8 \times 10^{-3}$	-5–4	0.5×10^3
	160	$4.9–7.0 \times 10^{-3}$	-3–2	10^3
5	25	$4.4–5.1 \times 10^{-4}$	-1–7	10^2
	120	0.03–0.05	-2–10	10^2
	140	0.05–0.08	-4–7	10^3
	160	0.09–0.1	-5–6	10^3
6	25	$1.4–2.0 \times 10^{-4}$	-1–1	10^2
	100	0.01–0.02	-4–5	10^3
	120	0.02–0.03	1–4	10^3
	140	$1.5–2.8 \times 10^{-2}$	-4– -1	10^3

[a] The performance data were obtained based on more than 10 OFET devices.

6. AFM images and XRD patterns of thin-films of 1, 2 and 4, 6

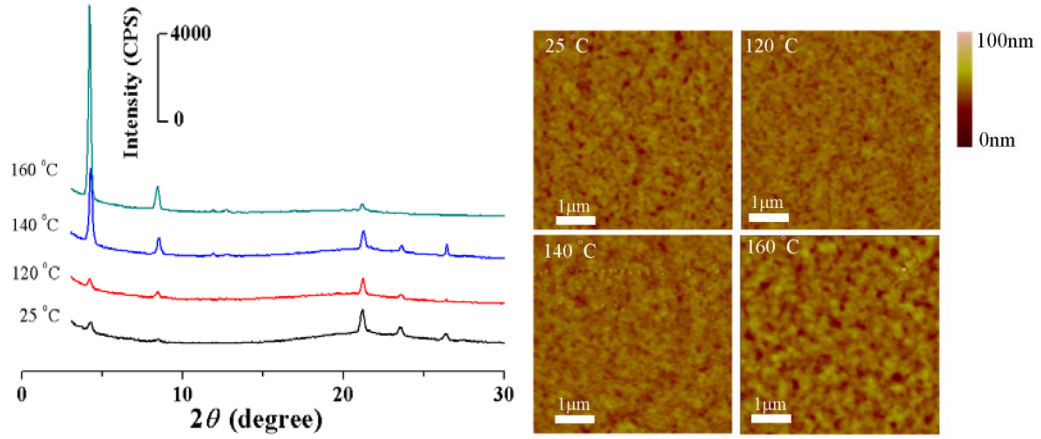

Figure S18. XRD patterns (*left*) and AFM images (*right*, on OTS modified Si substrate with taping mode) of **1** at different annealing temperatures.

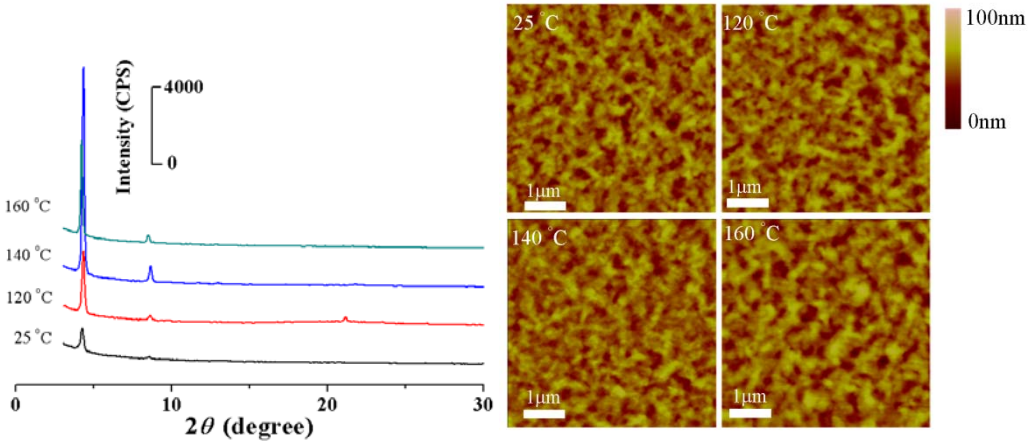

Figure S19. XRD patterns (*left*) and AFM images (*right*, on OTS modified Si substrate with taping mode) of **2** at different annealing temperatures.

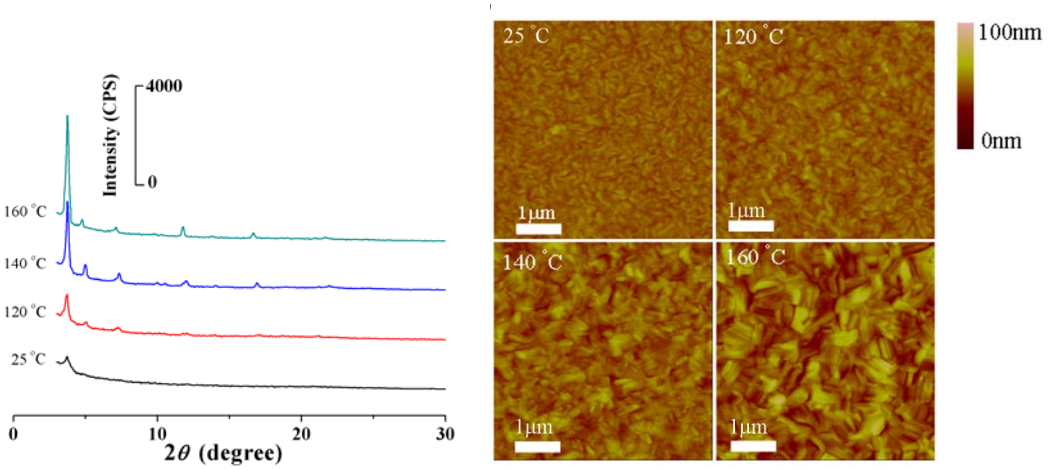

Figure S20. XRD patterns (*left*) and AFM images (*right*, on OTS modified Si substrate with taping mode) of **4** at different annealing temperatures.

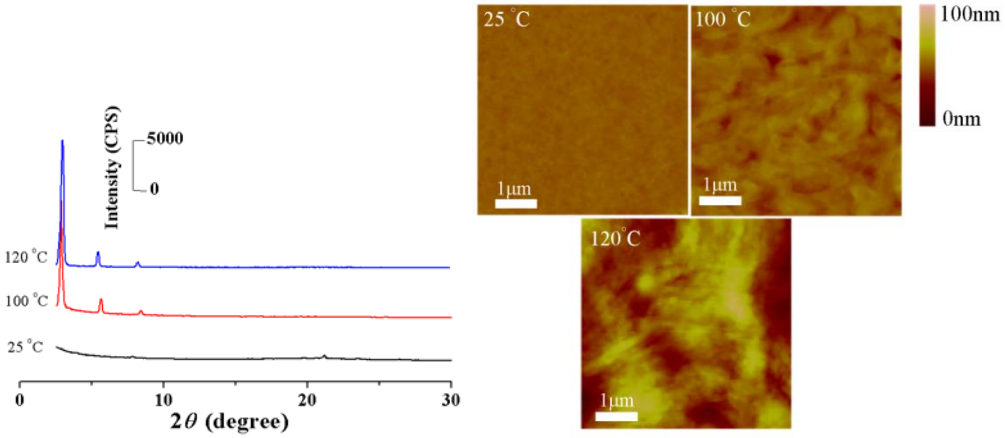

Figure S21. XRD patterns (*left*) and AFM images (*right*, on OTS modified Si substrate with taping mode) of **6** at different annealing temperature.

7. DFT calculation data

Calculation method: B3LYP/6-31G (d, p) with Gaussian 09

Data for compounds **1-3**:

		Coordinates		
		X	Y	Z
1	C	-0.58618	-0.6957	-1.1152
2	C	-0.57974	0.742165	-1.06435
3	C	-1.78373	1.429124	-0.84491
4	C	-2.9763	0.722692	-0.53586
5	C	-2.98319	-0.69199	-0.5882
6	C	-1.79694	-1.3853	-0.94695
7	C	-4.15663	1.416068	-0.16356
8	C	-5.31259	0.710325	0.170687
9	C	-5.31978	-0.70933	0.117113
10	C	-4.17057	-1.39952	-0.26883
11	C	-4.20089	-2.87181	-0.32369
12	N	-3.04526	-3.5076	-0.76171
13	C	-1.88582	-2.84676	-1.18396
14	C	-1.85957	2.90469	-0.97561
15	N	-3.01127	3.5437	-0.50169
16	C	-4.17214	2.888522	-0.10816
17	S	-0.99786	-3.48521	-1.73271
18	C	-5.20812	-3.50364	-0.0155
19	C	-5.17215	3.505642	0.249395
20	S	-0.96768	3.573237	-1.48039
21	S	-3.0643	-4.96892	-0.92825

22	C	-3.01671	5.013435	-0.56055
23	S	0.888269	-1.64396	-1.50998
24	C	2.128361	-0.67128	-0.72002
25	S	2.135014	0.667672	-0.67575
26	C	0.90279	1.702224	-1.39609
27	C	3.385942	-1.52655	0.205249
28	S	4.368667	-0.0502	0.409244
29	O	3.402755	1.447254	0.301667
30	O	5.698169	-0.06571	0.644849
31	O	6.670829	1.401136	0.900394
32	O	8.245091	0.59558	0.652971
33	C	8.237389	-0.75782	0.619984
34	C	6.656787	-1.55927	0.786923
35	H	9.679168	1.629121	0.598821
36	H	9.619289	-1.8506	0.408525
37	H	9.531295	2.356684	-1.08201
38	H	10.50554	-1.65654	2.004635
39	H	-6.80852	1.493767	0.676504
40	H	-7.69035	-0.01567	0.888394
41	S	-6.82388	-1.51363	0.562393
42	S	-9.00636	-0.02449	1.296104
43	C	-9.71306	-1.2522	1.466676
44	C	-9.70069	1.193781	1.559702
45	C	-10.2728	-2.26488	1.600063
46	C	-10.2501	2.199054	1.769879
47	N	-3.94974	-5.34909	-0.42581
48	N	-3.09338	-5.22522	-1.98979
49	S	-2.15678	-5.38882	-0.49456
50	S	-2.10477	5.391992	-0.09894
51	C	-3.89788	5.363815	-0.02975
52	H	-3.04478	5.347159	-1.60036
53	H	10.35361	3.069738	-1.17268
54	H	8.582069	2.882277	-1.19497
55	C	9.633031	1.581039	-1.84194
56	H	11.31488	-2.39016	1.982353
57	H	10.92511	-0.65422	2.094906

Total energy: 7447.0052061542 Hartrees

Data for compounds **4-6**:

		Coordinates		
		X	Y	Z
1	C	2.447844	-2.08417	1.008677

2	C	2.447748	-2.25621	-0.4149
3	C	1.239755	-2.53279	-1.0734
4	C	0.000591	-2.45781	-0.38081
5	C	0.000367	-2.28781	1.022709
6	C	1.239391	-2.19546	1.713575
7	C	-1.23837	-2.53115	-1.07392
8	C	-2.44647	-2.25407	-0.4159
9	C	-2.4471	-2.08305	1.007811
10	C	-1.23893	-2.19497	1.713069
11	C	-1.23463	-2.25751	3.192733
12	N	-0.00013	-2.16335	3.835261
13	C	1.234695	-2.2578	3.193285
14	C	1.235871	-2.94596	-2.49555
15	N	0.00112	-3.00703	-3.14181
16	C	-1.23362	-2.94274	-2.49635
17	S	-3.96723	-2.23601	-1.37917
18	C	-4.87461	-0.99137	-0.52036
19	C	-4.87629	-0.83331	0.809756
20	S	-3.96925	-1.84044	1.938366
21	S	-5.73083	0.231615	-1.49115
22	C	-6.58719	0.895562	-0.07244
23	S	-5.73523	0.582079	1.464588
24	C	-7.74442	1.585867	-0.15559
25	S	-8.58889	2.274383	1.253142
26	C	-10.1358	2.524238	0.407194
27	C	-10.133	2.358914	-0.93678
28	S	-8.56611	1.950977	-1.69069
29	O	2.255737	-2.41842	3.850642
30	O	2.257452	-3.25872	-3.09488
31	O	-2.25455	-3.25252	-3.09842
32	O	-2.25572	-2.41802	3.850057
33	C	-0.00119	-2.23088	5.303945
34	C	-0.0021	-3.42542	-4.55119
35	H	0.901193	-1.74476	5.667576
36	H	-0.89686	-1.73213	5.667294
37	H	-0.00892	-3.27058	5.642997
38	H	-0.03631	-4.51568	-4.63031
39	H	0.911775	-3.06254	-5.01557
40	H	-0.88535	-3.00788	-5.02951
41	S	-11.5072	2.951095	1.448747
42	S	-11.5022	2.643135	-2.01835
43	C	-11.8028	4.703865	0.989761
44	H	-12.172	4.779935	-0.03337
45	H	-12.5683	5.06437	1.680966

46	H	-10.8941	5.293436	1.119424
47	C	-11.8715	0.936756	-2.5911
48	H	-12.6765	1.035241	-3.32266
49	H	-10.9992	0.49028	-3.07038
50	H	-12.2076	0.319162	-1.75735
51	S	3.969723	-1.84098	1.939562
52	S	3.969252	-2.23975	-1.37713
53	C	4.876887	-0.83442	0.810543
54	C	4.875853	-0.99377	-0.51942
55	S	5.731815	0.228726	-1.49104
56	S	5.734768	0.582066	1.464383
57	C	6.587133	0.894623	-0.07262
58	C	7.743931	1.585625	-0.15596
59	S	8.566046	1.949789	-1.69106
60	S	8.587339	2.276092	1.252468
61	C	10.13442	2.526197	0.406939
62	C	10.13238	2.359547	-0.93687
63	S	11.50507	2.955093	1.448668
64	S	11.50182	2.643559	-2.01816
65	C	11.79963	4.707568	0.987941
66	H	12.16928	4.782789	-0.03512
67	H	10.89052	5.296667	1.116599
68	H	12.56468	5.069323	1.679078
69	C	11.87275	0.936753	-2.58855
70	H	11.00102	0.488923	-3.06757
71	H	12.67794	1.034957	-3.31993
72	H	12.20904	0.320535	-1.75386

Total energy: 10618.3959634218 Hartrees

8. ^{1}H NMR and ^{13}C NMR spectra of 1-6

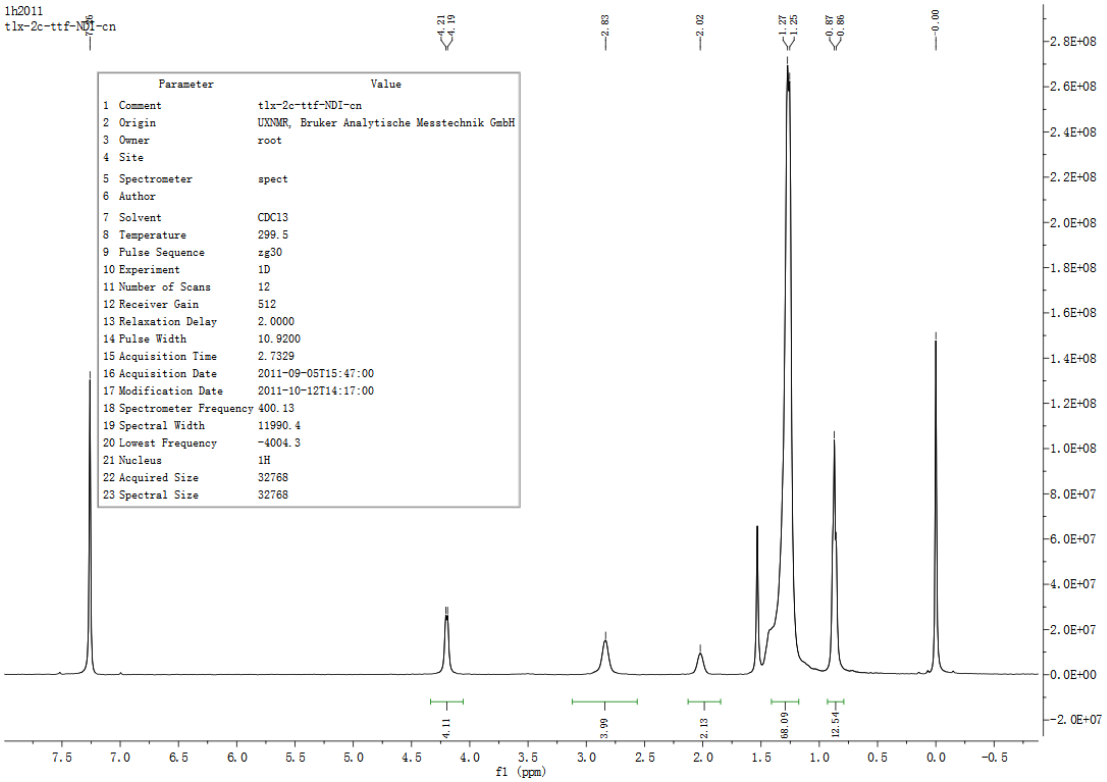

Figure S22. ^{1}H NMR spectrum of **1**

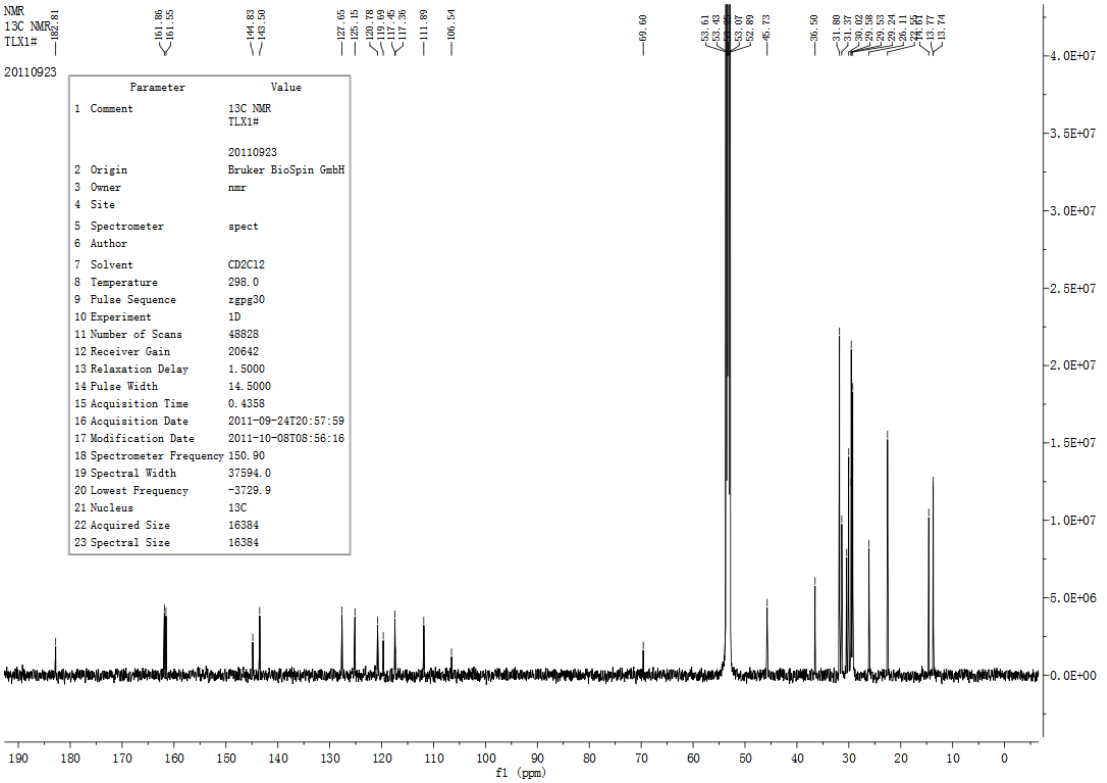

Figure S23. ^{13}C NMR spectrum of **1**.

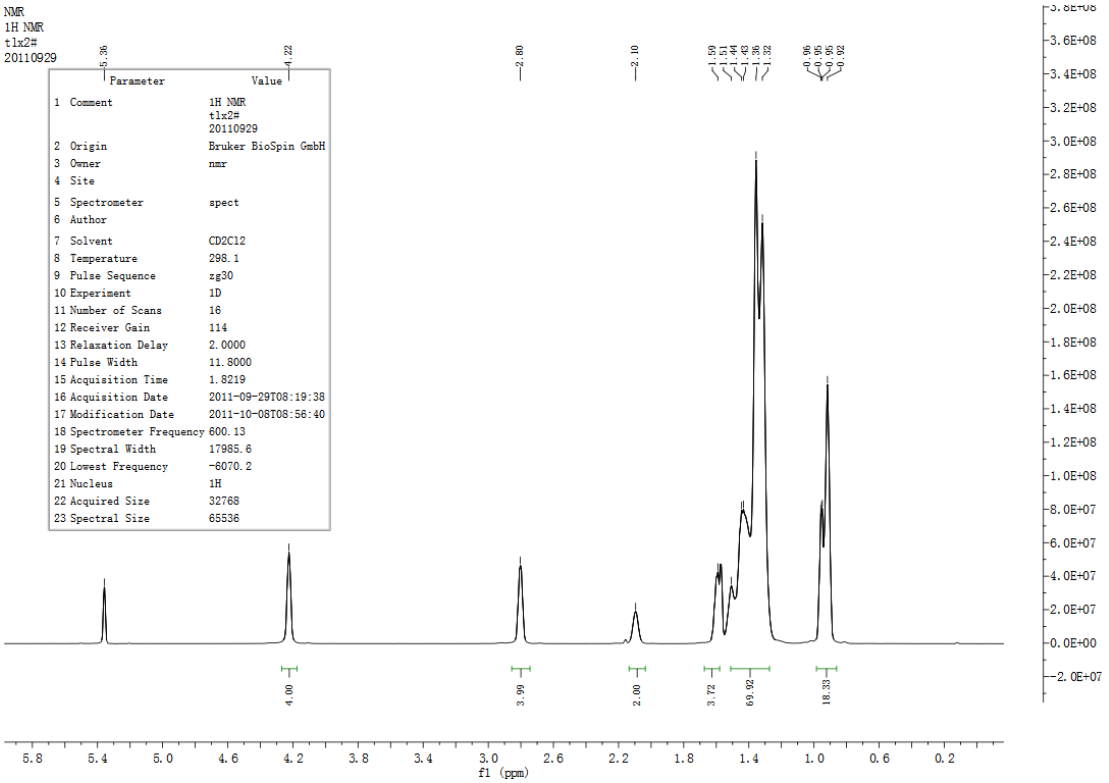

Figure S24. ^{1}H NMR spectrum of **2**

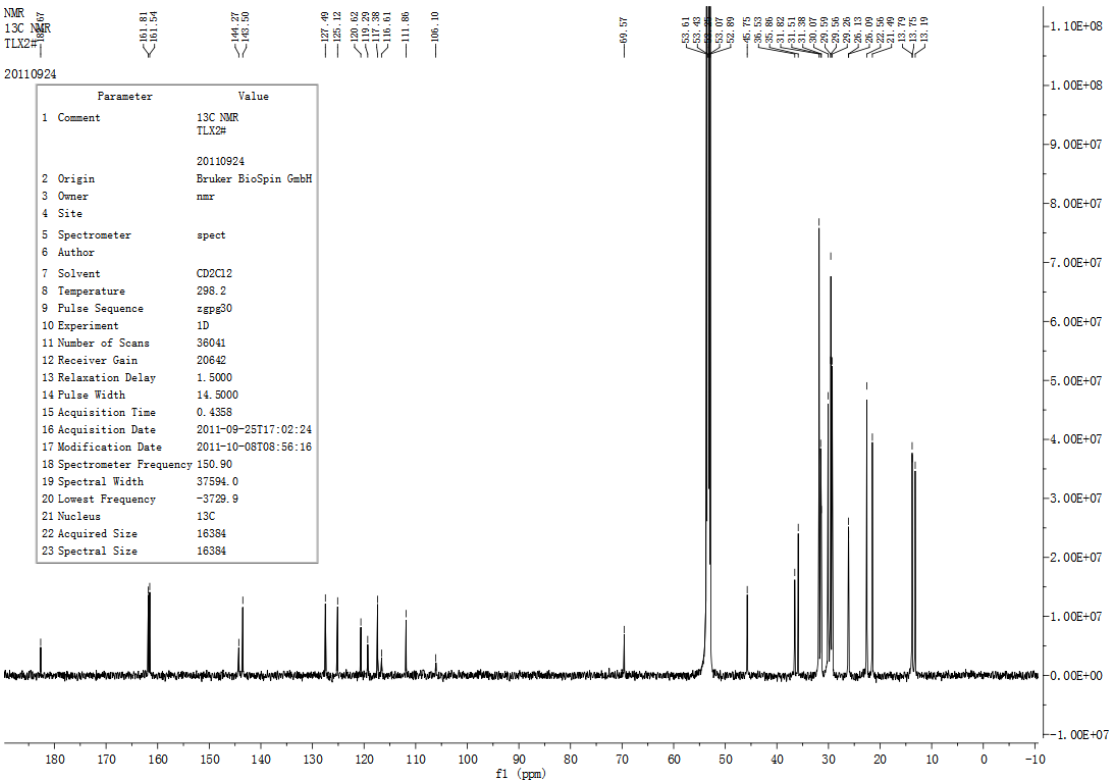

Figure S25. ^{13}C NMR spectrum of **2**.

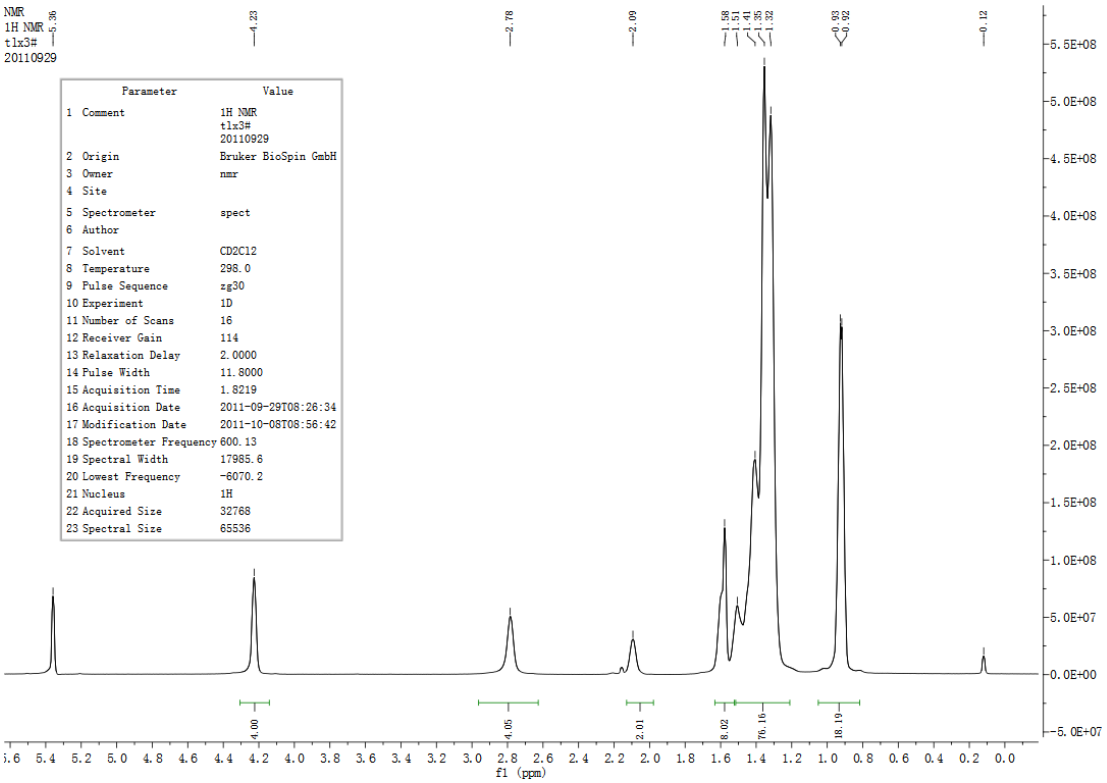

Figure S26. ^{1}H NMR spectrum of **3**

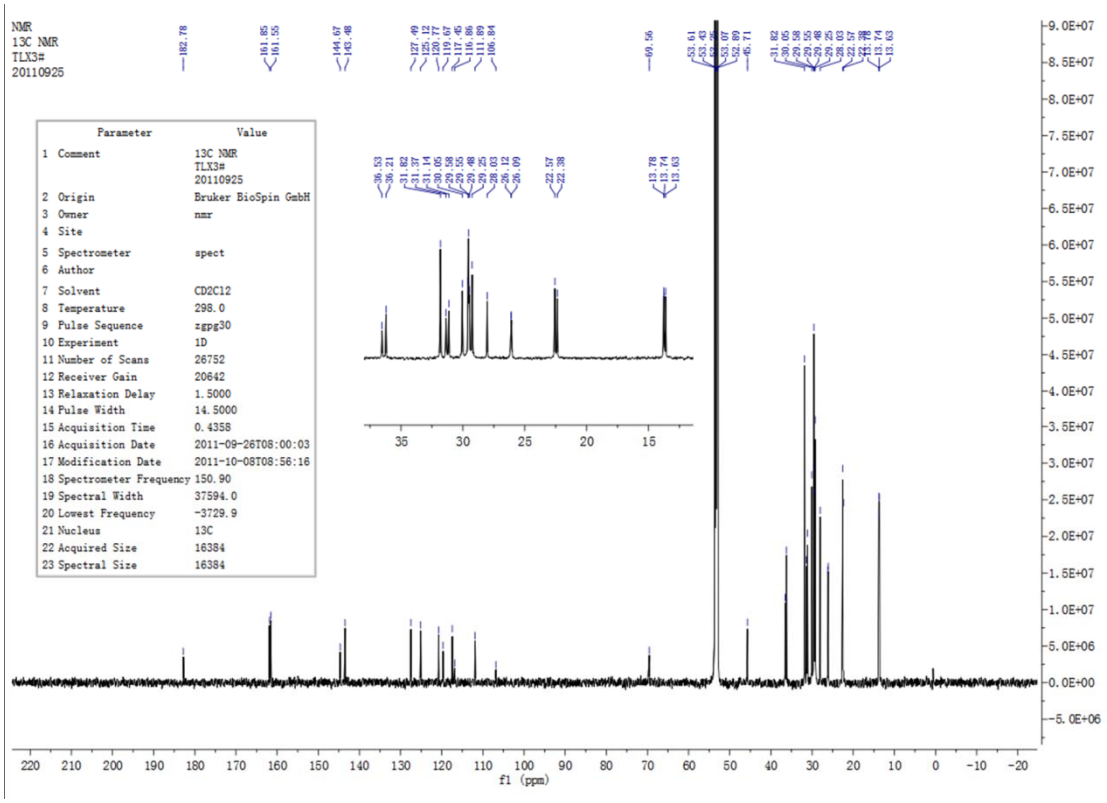

Figure S27. ^{13}C NMR spectrum of **3** (inset shows the details of the high field section).

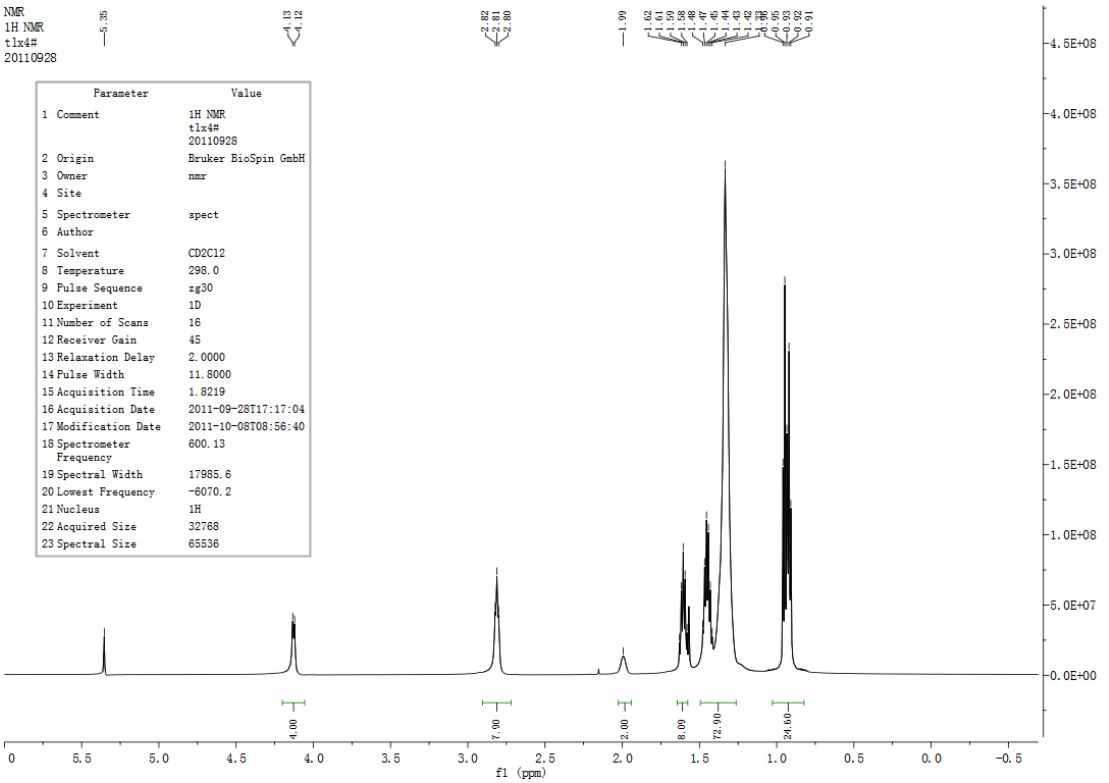

Figure S28. ^{1}H NMR spectrum of **4**

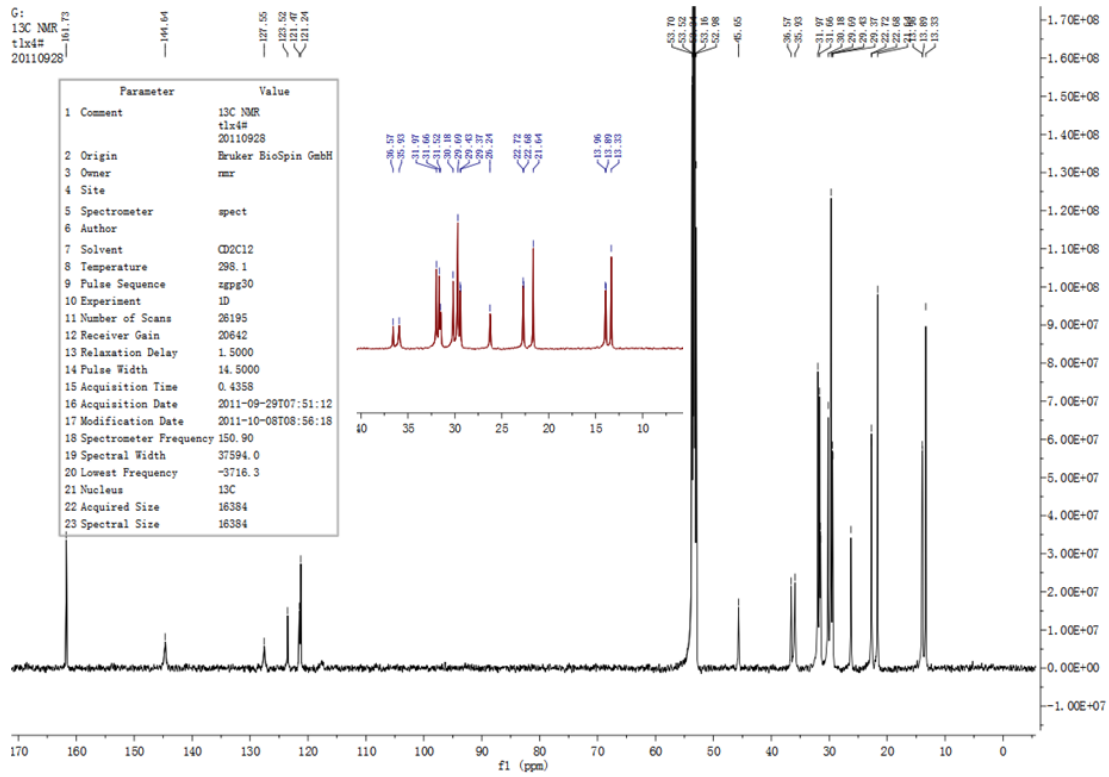

Figure S29. ^{13}C NMR spectrum of **4** (inset shows the details of the high field section).

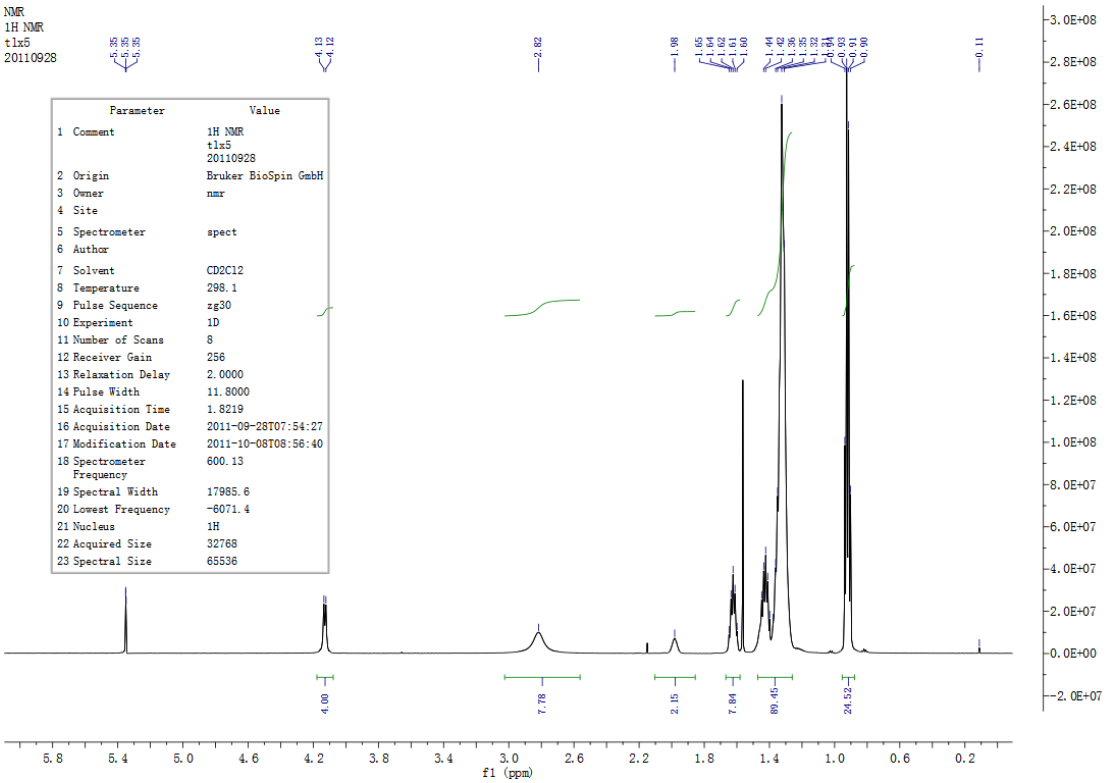

Figure S30. ^{1}H NMR spectrum of **5**

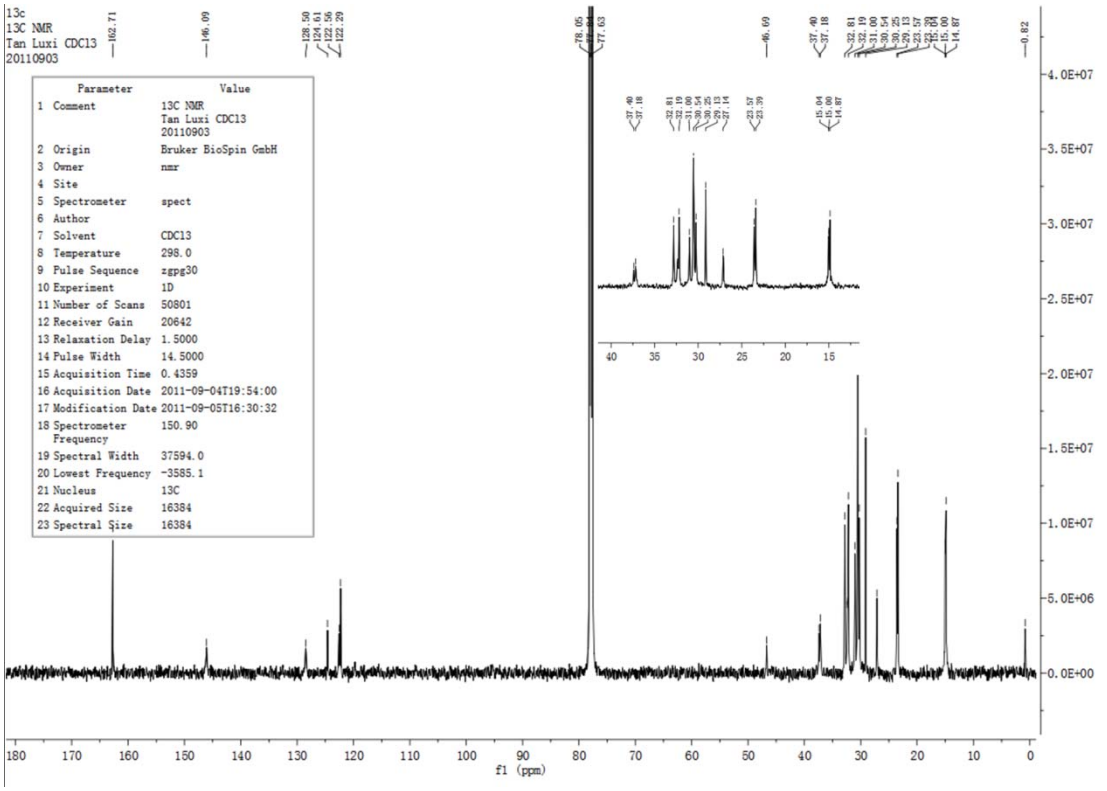

Figure S31. ^{13}C NMR spectrum of **5** (inset shows the details of the high field section).

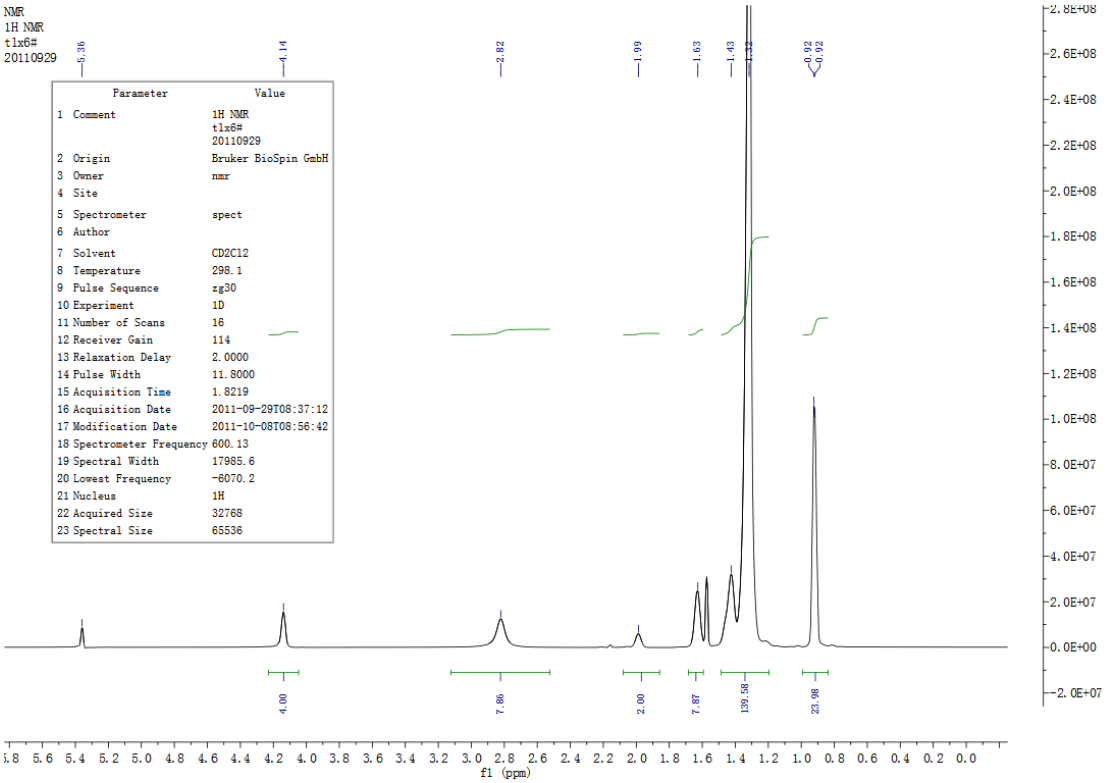

Figure S32. ^{1}H NMR spectrum of **6**.

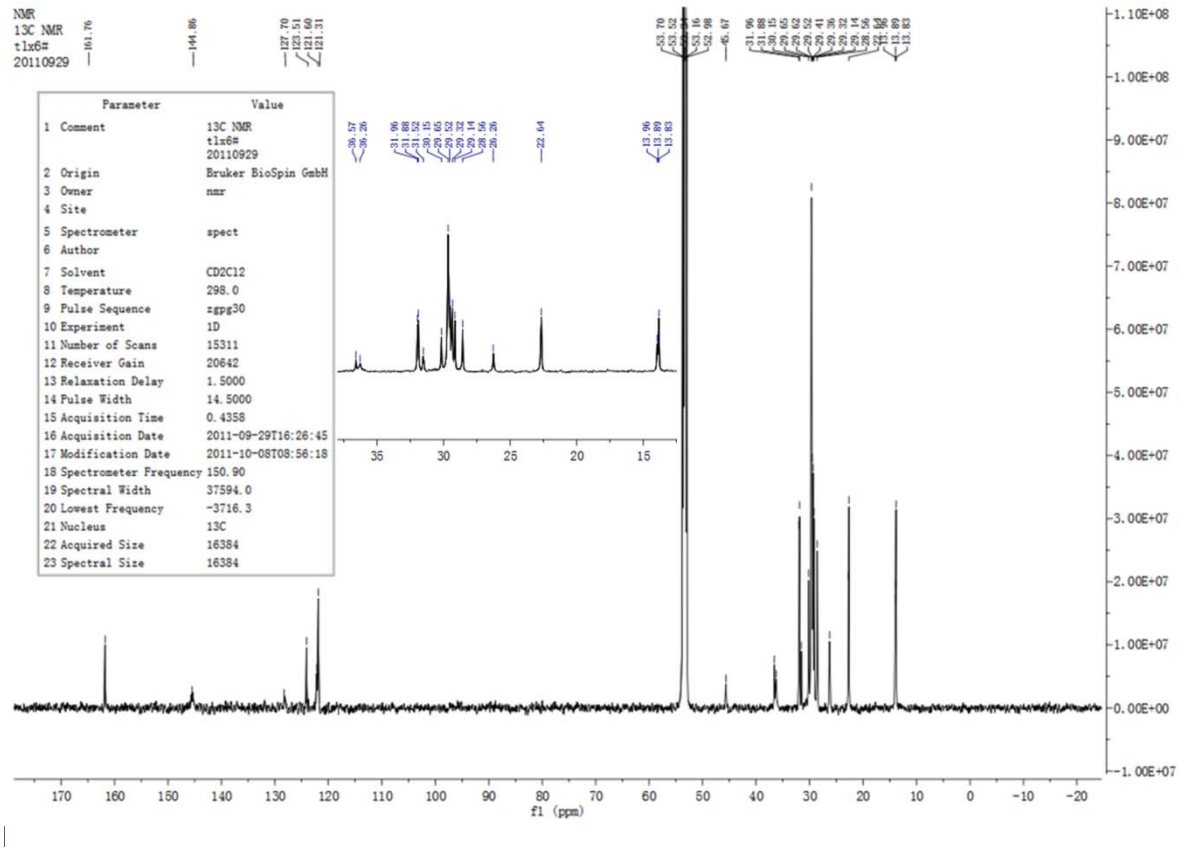

Figure S33. ^{13}C NMR spectrum of **6** (inset shows the details of the high field section).

9. The absorption spectra of compounds 2 and 4 after UV light irradiation

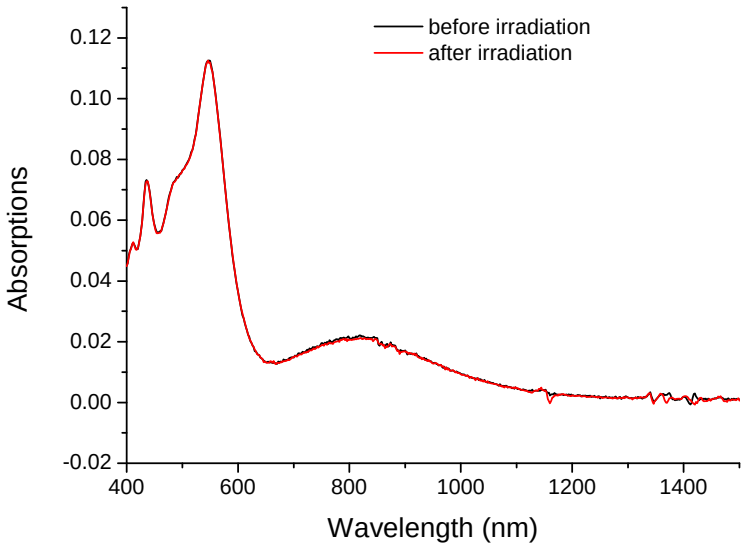

Figure S34. Absorption spectra of compound **2** in CH_2Cl_2 (~10^{-5} M) before and after UV light irradiation for 30.0 min (with a light source of wavelength: 365 nm, power: 8.0 mW, 5.0 cm away from the sample).

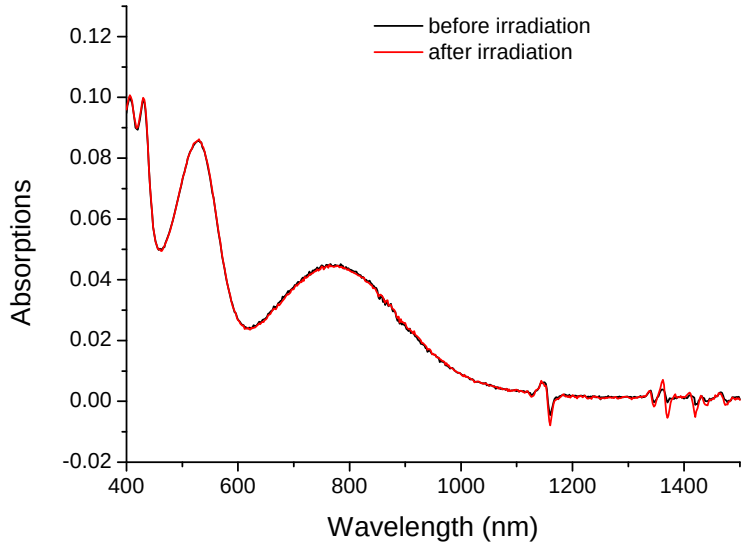

Figure S35. Absorptions of compound **4** in CH_2Cl_2 (~10^{-5} M) before and after UV light irradiation for 30 min. (with a light source of wavelength: 365 nm, power: 8.0 mW, 5.0 cm away from the sample).